International Journal for Research in Engineering Application & Management (IJREAM)
ISSN : 2454-9150 Vol-07, Issue-04, JULY 2021

# Fuzzy Control Improve Grid synchronization of Micro Grid Distributed WEC-PV-BEC Based Generation System

**K.G. Ravi Krishna, B.Tech. Student, EEE Department, Chadalawada Ramanamma Engineering College, Tirupati, Andhra Pradesh, India, kgravikrishna15@gmail.com**

**Dr. J. Srinu Naick, Professor, EEE Department, Chadalawada Ramanamma Engineering College, Tirupati, Andhra Pradesh, India, speaksrinu@gmail.com**

**Abstract—This paper proposes improve For a solar photovoltaic (PV)-wind-battery energy storage (BES) based micro grid system, the grid synchronisation of a renewable (Solar and Wind) energy sources based distributed generation system (DGS) is controlled to operate in the grid connected mode and an islanded mode using the Mamdani-fuzzy logic controller (FLC).An expert speed controller based on Mamdani-fuzzy logic controller (FLC) has been developed for a solar photovoltaic (PV)-wind-battery energy storage (BES) based micro grid system. The proportional and integral gains of the proportional integral (PI) controller are tuned by the Mamdani FLC. During dynamic situations, the traditional PI controller suffers from excessive overshoot and narrow bandwidth. These problems are overcome by fine-tuning the controller gains on a regular basis. The Mamdani adapted PI controller takes the speed error and the change in speed error as input and provides the adjusted gain parameters of the PI controller according to the operating conditions. For maximum power extraction, the double-stage solar PV array with intermediate boost converter employs an incremental conductance (InC) MPP method. The flexible power flow is allowed by using a battery at the DC link. A prototype is developed in the laboratory and tested in accordance to IEEE519 standard under steady state and dynamic conditions including variable wind speeds, changing insulation and load unbalanced conditions.**

***Keywords —Distributed Generation System, Load converter, Machine Converter, photovoltaic, Power Quality, Synchronization.***

## I. INTRODUCTION

Due to the abundance of renewable energy sources (RESs), distributed generation systems (DGSs) based on RESs are gaining traction now a day's [1]-[2]. Environmental concerns caused by the retirement of fossil fuel power facilities have fueled the expansion of RES-based DGS. Due to the intermittent nature of RES such as solar and wind, the RES-based DGS faces various issues, such as voltage and frequency fluctuations in an islanded mode [3]. As a result, in the islanded mode of operation, the storage battery is introduced in the RES based DGS. The importance of a storage battery in an islanded DGS has been reported by Alsaidan et al. [4] and Datta et al. [5]. As a result, RES-based DGSs can provide high-quality power to local loads. Despite its many positive attributes, the DGS is still a young technology. Various control and operational challenges, such as grid synchronization control in grid-connected mode, stability and reliability, power management, and voltage control in islanded mode [6]-[10], are thoroughly investigated. Various grid synchronization approaches are described in the literature [11]-[14] in order to increase control performance and inject high quality power into the grid. In multifunctional DGS, the accurate phase angle detection approach plays a critical role in the grid synchronization unit. Various phase angle detection techniques have been published in the preceding few decades, including SRF-PLL (Synchronous Reference Frame- Phase Locked Loop), ANF (Adaptive Notch Filter) [13], and CDSC-PLL (Cascaded Delayed Signal Cancelation) [14]. When input voltages are distorted and imbalanced, these reported techniques use a phase angle detection methodology. However, under nonlinear loading, this technique ignores the mode of transitioning from an islanded to a grid-connected state. The MSOS–FLL (Modified Second Order Sequence Frequency Locked Loop) is utilized to estimate the phase angle of the grid

 DOI : 10.35291/2454-9150.2021.0414 © 2021, IJREAM All Rights Reserved.

voltage in the proposed DGS, and an individual synchronization mechanism is employed to quickly move from an islanded mode to a grid linked mode and vice versa. This phase angle estimator performs well when frequency varies, which is useful in the MSOS-FLL. A new grid-connected control is also presented to improve the performance of DGS in the grid-connected mode of operation under dynamic situations, in addition to the synchronization technique.

The switching pulses for the grid-connected VSC (Voltage Source Converter) are typically generated using an indirect current control [15]. The indirect control has been mentioned extensively in the literature [16]-[21]. The reference grid currents in a solar grid-connected system are estimated using the fundamental load current and other feed forward terms in an indirect current control. The filter used to determine the load current fundamental for reference grid current calculation was explained by Vishal et al. [17]. The disclosed control strategies, on the other hand, have a few advantages over other control systems. SRF (Synchronous Reference Frame) [17] based control techniques are resilient and fast in normal conditions, but their performance is harmed by DC-offset conditions and imbalanced load currents. Similarly, control approaches based on PLL, EPLL [18], SOGI [19], advanced SOGI-PLL [20], and SOGI-FLL [21] have some advantages and disadvantages. In the grid-connected mode, this paper uses an IAPV (Improved Affine Projection Versoria) based adaptive VSC control algorithm with an improved feed-forward term [22]-[23]. The IAPV has a number of advantages over existing control methods.

In addition to a quick, adaptive, and resilient grid-connected filter, an improved feed-forward term is provided to increase the system's dynamic response. The primary goal of the IAPV control algorithm in grid-connected mode is to estimate balanced and sinusoidal reference grid currents regardless of grid voltage operating conditions. In addition, in the islanded mode of operation, the VSC (LC-Load Converter) control switches to voltage control mode, which is based on PR (Proportional Resonant) rather than PI (Proportional Integral) control? Because PI control's response and tracking capabilities are insufficient for AC amounts. As a result, the focus of this paper is on multifunctional and multi-objective DGS. An extensive literature survey [24]-[44] has been included in Table I to illustrate the paper's key contribution. The following are the primary contributions of this work.

- Based on grid availability and grid failure, this distributed generation system (DGS) is run in an islanded mode and a grid-connected mode.
- The MSOS-FLL based phase angle estimator is utilised in the synchronisation unit to improve grid synchronisation and to protect the synchronisation process from voltage distortion and frequency variation.
- The revised affine projection versoria control algorithm is employed in grid-connected mode to inject solar and wind-generated active energy into the grid with improved power quality. In addition, the grid currents are insulated from DC-offset and load current harmonics.
- In grid-connected mode, the solar power feed-forward term is employed to increase DGS' dynamic reaction to fast and sudden changes in solar irradiation.
- In the event of a grid fault, the DGS shifts to an islanded mode without any transitory. The PR controller is used to achieve balanced and sinusoidal CCP (Common Coupling Point) voltages in an islanded mode of operation of DGS. As a result, CCP voltages' power quality is always well within the IEEE-1547 standard.

## II. DGS CONFIGURATION

A DGS (Distributed Generation System) with a solar PV (Photovoltaic) array, a wind turbine-driven SCIG (Squirrel Cage Induction Generator), and an energy storage battery is shown in Figure 1. As indicated in Fig. 1, the grid is connected to DGS's CCP (Common Coupling Point) using solid state switches (Solid State Switches). The boost converter connects the solar PV array to the LC (Load Converter (DC-link )'s and provides the solar-generated active power to the DC-link. MC is used to regulate the SCIG wind turbine (Machine Converter). As indicated in Fig. 1, two R-C filters are utilised to eliminate switching noise from the CCP voltages.

## III. CONTROL STRATEGY

To alter the DGS mode, the converter control approach is employed. In this application, two converters are used: one for generator control and the other for load/grid power control. The load side converter (LC) regulates the islanded micro grid's voltage and frequency, as well as grid connection/disconnection control and grid power quality, in grid connected mode. The machine converter extracts the peak power from the wind generator while simultaneously monitoring the generator current quality. To ensure that local loads receive uninterrupted power, this DGS operates in both grid-connected (GC) and islanded mode (IM).This paper presents a robust control technique for operating DGS in IM and GC modes without any transients.

This work shows how to operate DGS in IM and GC modes without any transients using a strong control method. The control strategy is broken down into three parts: (1) grid-connected mode (as shown in Fig. 2), (2) islanded

 DOI : 10.35291/2454-9150.2021.0414 © 2021, IJREAM All Rights Reserved.

mode, and (3) synchronization control. For active power balancing, a storage battery is employed in this DGS, which is coupled to the DC-link through a bi-directional DC-DC converter (BDC). The BDC's job in this DGS is to maintain the battery current safe even when the second harmonic is present by controlling the DC-link voltage as shown in Fig. 3. The control algorithm of the DGS is detailed in the following subsections.

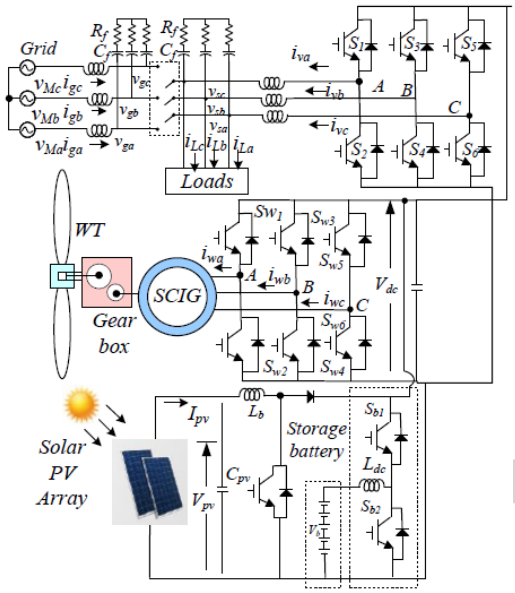


**Fig. 1 Distributed generation system configuration**

*A. Grid-Connected Mode of DGS*

The LC switching pattern is generated using an indirect current control in grid-connected mode. The IAPV (Improved Affine Projection Versoria) algorithm is used to control the indirect current of LC, as shown in Fig.2 (a). The IAPV filter is used to estimate reference grid currents to improve grid current quality for highly nonlinear loads. The load current fundamental component is estimated using the IAPV approach. The IAPV control method requires the in-phase component to determine the load current basic component, as shown in Fig. 2. (a). A formula for estimating in-phase unit templates is as follows:

$$u_a = \frac{v_{ga}^{+}}{V_t}, u_b = \frac{v_{gb}^{+}}{V_t}, u_c = \frac{v_{gc}^{+}}{V_t} \quad (1)$$

Where, vga, vgband vgcare grid phase voltages. The grid phase voltages are computed through the following expression,

$$v_{ga}^{+} = \frac{1}{3}\left(2v_{gab}^{+} + v_{gbc}^{+}\right), \quad v_{gb}^{+} = \frac{1}{3}\left(-v_{gab}^{+} + v_{gbc}^{+}\right),$$
$$v_{gc}^{+} = \frac{1}{3}\left(-v_{gab}^{+} - 2v_{gbc}^{+}\right) \quad (2)$$

Where, vgab+, vgbc+ are the positive sequence line voltages and these positive sequence voltages are estimated using the MSOS (Modified Second Order Sequence)-FLL as shown in Figs. 3-4 and following governing equations.

$$v_{gab}^{+} = \frac{1}{3}\left[\frac{1}{2}\left(v_{gbc} - v_{gca}\right) + v_{gab}\right] - \left[\frac{1}{2\sqrt{3}}\left(v_{gbc} + v_{gca}\right)\right] \quad (3)$$

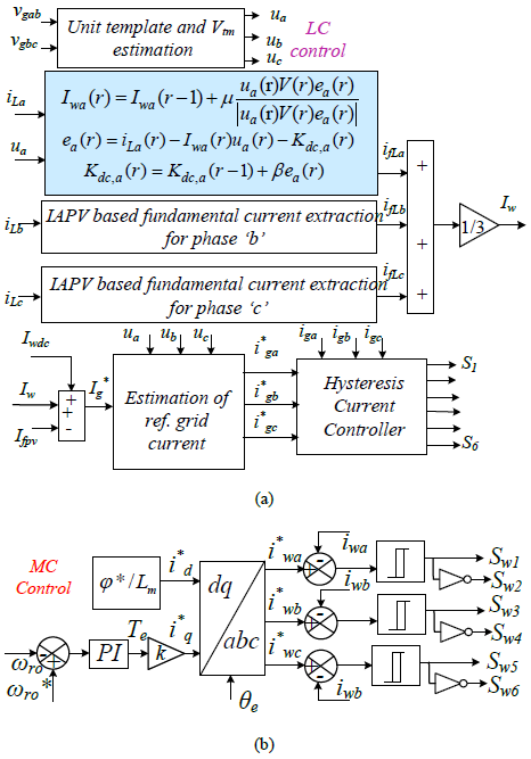


**Fig.2 Grid connected control (a) for LC and (b) for MC**

$$v_{gca}^{+} = \left[\frac{1}{2\sqrt{3}}\left(v_{gab} - v_{gbc}\right)\right] - \frac{1}{3}\left[\frac{1}{2}\left(v_{gab} + v_{gbc}\right) + v_{gca}\right] \quad (4)$$

$$v_{gbc}^{+} = \left(-v_{gab}^{+} - v_{gca}^{+}\right) \quad (5)$$

Where, vgab+, vgbc+ and vgca+ are the positive sequence voltages. The fundamental active current component is estimated as [45],

$$I_{pa}(r) = I_{pa}(r-1) + \mu \frac{u_a(r)V(r)e_a(r)}{|u_a(r)V(r)e_a(r)|} \quad (6)$$

$$\text{Where } e_a(r) = i_{La}(r) - I_{pa}(r)u_a(r) - K_{dc,a}(r) \quad (7)$$

and μ is equal to .0025.

$$\text{And } K_{dc,a}(r) = K_{dc,a}(r-1) + \beta e_a(r) \quad (8)$$

Where, Kdc,a is an adaptive variable to reject the DC-offset component. Similarly, the active weight components of load currents for phase 'b' and 'c' are estimated as,

$$I_{pb}(r) = I_{pb}(r-1) + \mu \frac{u_b(r)V(r)e_b(r)}{|u_b(r)V(r)e_b(r)|} \quad (9)$$

 DOI : 10.35291/2454-9150.2021.0414 © 2021, IJREAM All Rights Reserved.

$$e_b(r) = i_{Lb}(r) - I_{pb}(r)u_b(r) - K_{dc,b}(r) \quad (10)$$

$$I_{pc}(r) = I_{pc}(r-1) + \mu \frac{u_c(r)V(r)e_c(r)}{|u_c(r)V(r)e_c(r)|} \quad (11)$$

$$e_c(r) = i_{Lc}(r) - I_{pc}(r)u_c(r) - K_{dc,c}(r) \quad (12)$$

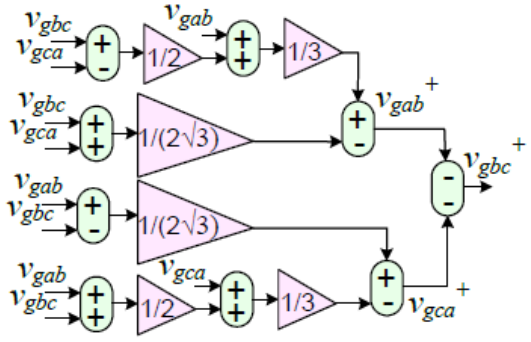


**Fig. 3 Positive sequence estimator**

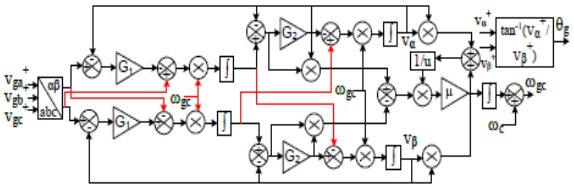

**Fig. 4 MSOS-FLL block diagram**

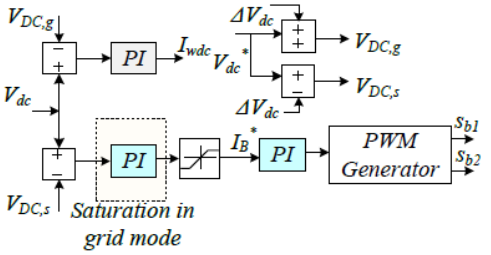


**Fig. 5 BDC and solar PV array peak power control**

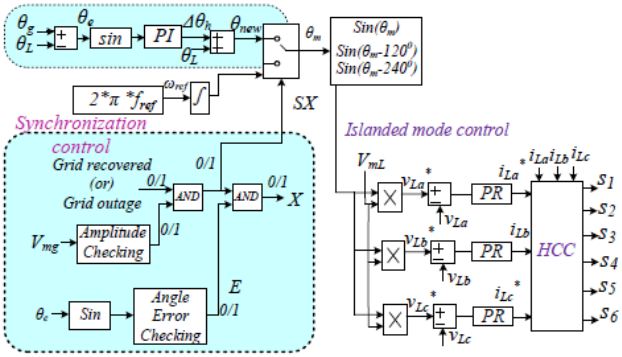


**Fig. 6 Islanded mode of LC control**

The average fundamental load current is estimated as,

$$I_p = \frac{I_{pa} + I_{pb} + I_{pc}}{3} \quad (13)$$

The reference grid current weight is computed as,

$$I_g^* = I_p + I_{dc} - I_{fpv} - I_{fwi} \quad (14)$$

Where, Idc is a weight component for DC-link voltage control. The common DC-link voltage is controlled through a PI controller, which is formalized in discrete time as,

$$I_{dc}(r) = I_{dc}(r-1) + k_p\{(V_e(r) - V_e(r-1)\} + k_i\{V_e(r)\} \quad (15)$$

Where, Ve is error of reference DC-link voltage (Vdc*) and the sensed DC-link voltage (Vdc).

Ifpv and Ifw are the PV power and wind power feed-forward terms, respectively. The PV feed-forward term is estimated as,

$$I_{fpv} = k\left(\frac{2P_{pv}}{3V_t}\right) \text{and } I_{fwi} = \left(\frac{2P_{wind}}{3V_t}\right) \quad (16)$$

Therefore, the response of the system is improved under dynamic condition. The reference sinusoidal grid currents are estimated as follows,

$$i_{ga}^* = u_a \times I_g^*, i_{gb}^* = u_b \times I_g^*, i_{gc}^* = u_c \times I_g^* \quad (17)$$

The hysteresis current controller is used to generate the switching pulses of LC. The hysteresis band error is calculated using reference and measured grid currents. The MC control for extracting the wind peak power with better SCIG power quality is shown in Fig. 2 (b). As shown in Fig. 2, the MC control is based on an indirect vector control (b). In addition, Fig. 5 depicts the DC-link voltage regulation technique in conjunction with the solar peak power extraction management algorithm. The BDC (Bidirectional DC-DC Converter) in islanded mode is used to regulate the DC-link voltage. In the grid-connected mode, however, an outside PI (Proportional Integrator) is saturated, and BDC switching pulses are obtained by using the constant current mode, while DC-link voltage control is performed by using

 DOI : 10.35291/2454-9150.2021.0414 © 2021, IJREAM All Rights Reserved.

the load converter. The outer PI controller is saturated in grid linked mode, and the battery reference current is equal to the lower saturation limit. The PI controller for battery current is written as,

$$D(r)=D(r-1)+k_{pib}\{I_{be}(r)-I_{be}(r-1)\}+k_{ppb}I_{be}\ (r) \quad (18)$$

Where, Ibe is error between the reference and sensed battery currents. These kpib and kppb are the gains of the PI controller.

*B. Islanded Mode of DGS*

The LC is employed to create the CCP voltages in the islanded mode using the PR (Proportional Resonant) controller, as shown in Fig. 6. The DSP (Digital Signal Processor) and reference voltage Vref = 230*2/(3)V and frequency (fref = 50Hz) provide the reference CCP voltage. The VSC control method in islanded mode comprises of three PR (Proportional Resonant) controllers. The outputs of PR controllers are written as [46],

$$i_{vsca}(\mathrm{r})=n_o v_{ea}(\mathrm{r})+\mathrm{n}_1 v_{ea}(\mathrm{r}-1)+\mathrm{n}_2 v_{ea}(\mathrm{r}-2)-\mathrm{d}_1 i_{vsca}(\mathrm{r}-1)-\mathrm{d}_2 i_{vsca}(\mathrm{r}-2) \quad (19)$$

$$i_{vscb}(k)=n_o v_{eb}(\mathrm{r})+\mathrm{n}_1 v_{eb}(\mathrm{r}-1)+\mathrm{n}_2 v_{eb}(\mathrm{r}-2)-\mathrm{d}_1 i_{vscb}(\mathrm{r}-1)-\mathrm{d}_2 i_{vscb}(\mathrm{r}-2) \quad (20)$$

$$i_{vscc}(\mathrm{r})=n_o v_{ec}(\mathrm{r})+\mathrm{n}_1 v_{ec}(\mathrm{r}-1)+\mathrm{n}_2 v_{ec}(\mathrm{r}-2)-\mathrm{d}_1 i_{vscc}(\mathrm{r}-1)-\mathrm{d}_2 i_{vscc}(\mathrm{r}-2) \quad (21)$$

Where, n0,n1,n2,d1 and d2 are given in [24].

$$\text{And } v_{ea}(r)=v^{*}_{sa}(\mathrm{r})-v_{sa}(\mathrm{r}) \quad (22)$$

$$v_{eb}(r)=v^{*}_{sb}(\mathrm{r})-v_{sb}(\mathrm{r}) \quad (23)$$

$$v_{ec}(r)=v^{*}_{sc}(\mathrm{r})-v_{sc}(\mathrm{r}) \quad (24)$$

Where, vsa*, vsb* and vsc* are the reference phase voltages and vsa, vsband vscare sensed CCP phase voltages. CCP phase voltages are estimated through line voltages, which are expressed as,

$$v_{sa}=\frac{1}{3}\left(2v^{+}_{sab}+v^{+}_{sbc}\right),\quad v_{sb}=\frac{1}{3}\left(-v^{+}_{sab}+v^{+}_{sbc}\right),\quad v_{sc}=\frac{1}{3}\left(-v^{+}_{sab}-2v^{+}_{sbc}\right) \quad (25)$$

Where, vsab+,vsbc+ and vsca+ are line voltages as shown in Figure. In an islanded control algorithm of VSC, the PR controllers give reference converter currents (ivsca, ivscb and ivscc). The hysteresis current controller is used to generate the VSC switching pulses.

*C. Modified Second Order Sequence (MSOS)–FLL based Synchronization Control*

If grid availability is confirmed, the islanded DGS is switched to grid-connected mode, as shown in Figs. 5. The calculation of grid voltages phase angles and islanded CCP voltages phase angles is the theory underpinning the grid synchronizer process. The DGS synchronization unit is used to synchronies the phase islanded DGS voltages and grid voltage phase angles. MSOS-FLL is used to estimate the phase angles of the grid and CCP voltages. The phase estimator technique is quick and can estimate phase angles even when grid voltages are skewed. Following the calculation of phase angles, a PI (Proportional Integral) controller is utilized to match the phase angles of grid and CCP voltages.

$$\Delta\theta_d(r)=\Delta\theta_d(r-1)+k_{ps}\{\theta_e(r)-\theta_e(r-1)\}+k_{is}\{\theta_e(r)\} \quad (26)$$

Where Δθd is the PI controller output and θe is the error of grid and standalone phase angle and it is expressed as,

$$\theta_e(r)=\theta_g(r)-\theta_s(r) \quad (27)$$

Where θg is the grid voltage angle and θs is the standalone voltage angle. The updated phase angle (θn) is given to the

standalone controller for generating the standalone voltage same as the grid voltage as shown in Fig. 5. Hence the new updated phase angle is as,

$$\theta_n(r)=\theta_s(r)+\Delta\theta_d(r) \quad (28)$$

Where θs is the islanded CCP voltages phase angle.

## IV. NEW PROPOSED CONTROL STRATEGY

*A. Analysis of Fuzzy Predictive Control*

Combination with smart intelligent control has been recommended to get good robustness to the rapid change and uncertainty of these variables, in addition to the development in prediction algorithms of variables that satisfy the required calculations. To obtain a hybrid control method, FPC can be formed by combining FLC with MPC. The theoretical study of this proposed model and its operation in all elements of the system is described in the following sections. First and foremost, in the inner and outer circuits of MSC control, the FOC design has been employed to construct a PI controller as a typical control scheme. Because typical PI controllers are fixed gain feedback controllers, they are unable to correct for process parameters such as KP and KI fluctuations. PI-controlled

 DOI : 10.35291/2454-9150.2021.0414 © 2021, IJREAM All Rights Reserved.

systems are also less responsive to real-time and relatively quick changes in wind speed. As a result, new robust controllers are becoming increasingly important for adhering to grid code standards and engineering suggestions. Intelligent control systems, such as FLC, are being used in recently developed ways to ensure proper system behavior and operation. When compared to standard control systems, FLC system technique can improve tracking performance for both grid and load coupled loads, whether linear or non-linear. The combination of an FLC system controller and an MPC creates a hybrid control system called Fuzzy Predictive Control (FPC), which minimizes overshoot and settling time while achieving quick output signal response. Figure 9 is a schematic diagram of the FLC system that was employed. Input and output variables are determined using the methods outlined in Chapter 4. The error e and the change of error e are the system's two input variables. The form of the rule base's membership functions determines how an FLC behaves.

The output of the FLC is used to create the FPC scheme in this part. As a result, the output should be the iq reference value, which will be used as an input by MPC. The membership function values are assigned to the linguistic variables using seven fuzzy subsets called: Negative Big (NB), Negative Small (NS), Zero(Z), Positive Small (PS) and Positive Big (PB). The signals e and Δeare selected as an input to FLC in all cases as shown in Figure 7, while the output values of isq(k) is the outputs of the FLC as shown in Figure 8. In MSC, the signal e is the error between the reference current signals i∗ sdand i∗ sqand actualcurrent signal of the system for both d and q circuits as mentioned respectively, Δeis the change in error in a sampling period of time. In the same manner described, the fuzzified inputs are fed to the interface engine which is mainly consists of fuzzy rule base and fuzzy implication sub blocks.

**Table-1 Rule base table of the Fuzzy Controller**

| e \de | NB | NS | Z | PS | PB |
|---|---|---|---|---|---|
| NB | NB | NB | NS | NS | Z |
| NS | NB | NS | NS | Z | PS |
| Z | NS | NS | Z | PS | PS |
| PS | NS | Z | PS | PS | PB |
| PB | Z | PS | PS | PB | PB |

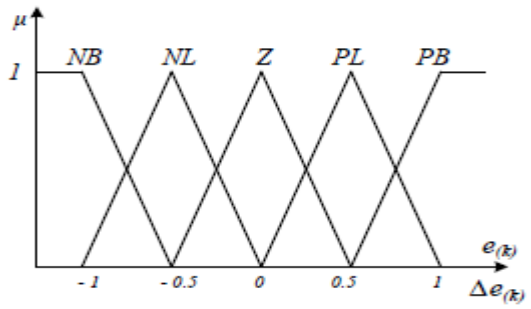


**Fig. 7 Membership Function of FLC for the input variables**

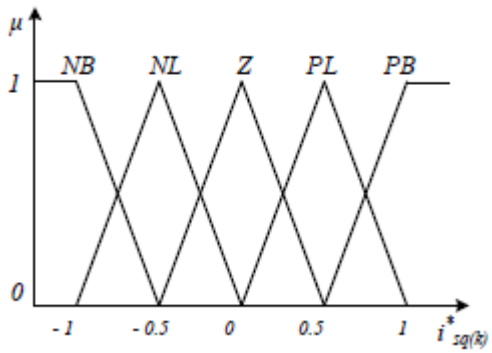


**Fig. 8 Membership Function of FLC for the output variables.**

The rule base is used at this stage to generate the output fuzzy set, which is then identified using the fuzzy implication approach. In the inference process, many approaches are used, such as the max-min implication methodology. Table-1 shows the interface fuzzy memory rules that apply to the proposed system. The output fuzzy range is located if the fuzzification procedure is complete. Defuzzification is required at this stage to transform the control signal's fuzzy value to a non-fuzzy value. In the proposed solution of the signals, the centroid defuzzification method is employed to reverse the fuzzification process.

*B. Structure of the Proposed Technique*

FLC's high performance allows designers to combine it with neural networks, genetic algorithms, adaptive and predictive controllers to boost output performance when the system's uncertainty parameters are high. The FPC system can control the output currents of both the generator and the grid while managing the system model. The suggested algorithm, MSC, was implemented using system controllers.

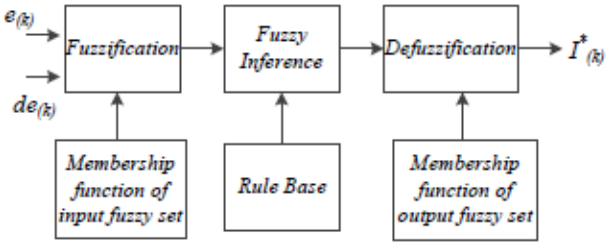


**Fig. 9 Structure of Fuzzy Logic Controller**

## V. RESULTS AND DISCUSSION

To demonstrate the effectiveness and robustness of the presented control, a DGS is developed in the laboratory as well as simulated in MATLAB/Simulink. The fast and accurate phase angle information is necessary for fast synchronization of the islanded micro grid to the grid. MSOS-FLL also improves the reference grid current estimation performance because the unit vector information is used in the reference grid current estimation and the MSOS-FLL algorithm obtains it by estimating the positive

 DOI : 10.35291/2454-9150.2021.0414 © 2021, IJREAM All Rights Reserved.

sequence voltages from the unbalanced and distorted voltages. The comparison of phase angle estimation performance at variable frequency using SRF-PLL, SOS-PLL and the MSOS-FLL. It is observed that at constant frequency, the performance of SRF-PLL, SOS-PLL and MSOS-FLL are similar. However, during the change in the frequency, the performance of MSOS-FLL is superior, and it is giving accurate phase angle information. comparison of synchronization performance using SRF-PLL and MSOS-FLL. It is observed that a synchronization of an islanded micro grid to the grid using MSOS-FLL is faster. Fig. 10(a) shows the seamless grid connection from an islanded to the grid connected mode. Fig. 10(b) shows the performance of the grid connected system at unbalanced load. Fig. 10(b) shows the battery current (Ib), grid current (ig), load current (iL), PV current (Ipv) and wind current (Iw). At unbalanced load, the battery current (Ib) is free from the second harmonic. Fig. 10(c) shows the response of DGS at solar insolation change and wind speed variation.

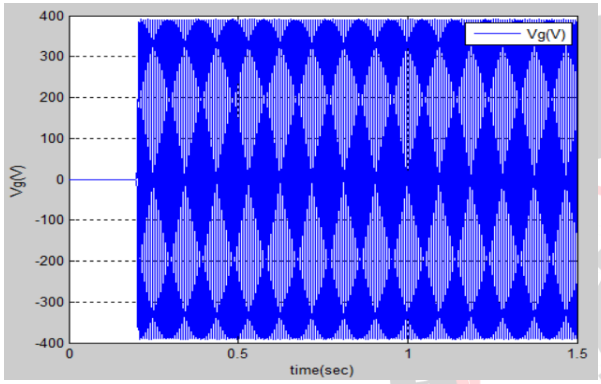


(a)

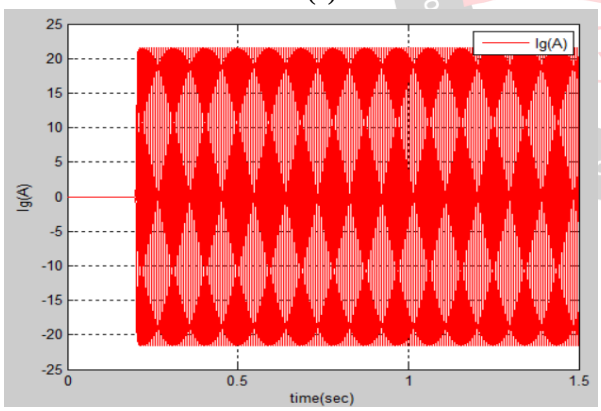


(b)

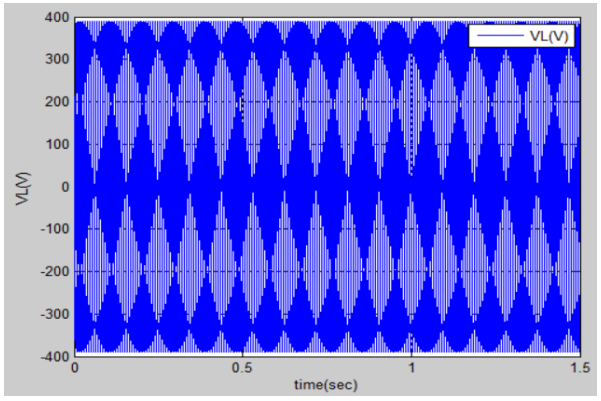


(c)

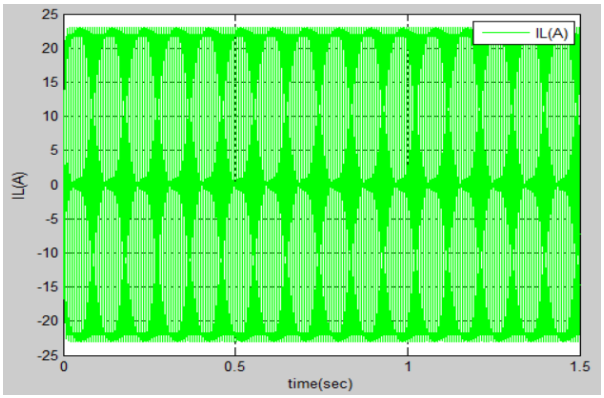


(d)

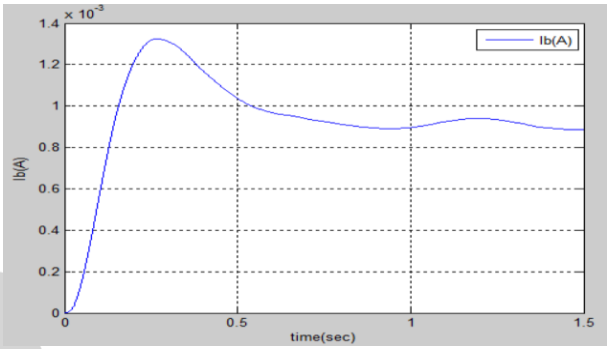


(e)

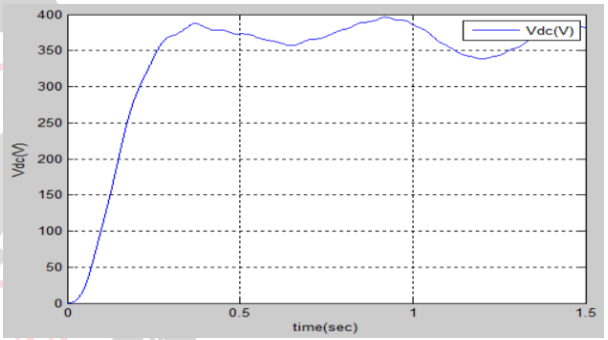


(f)

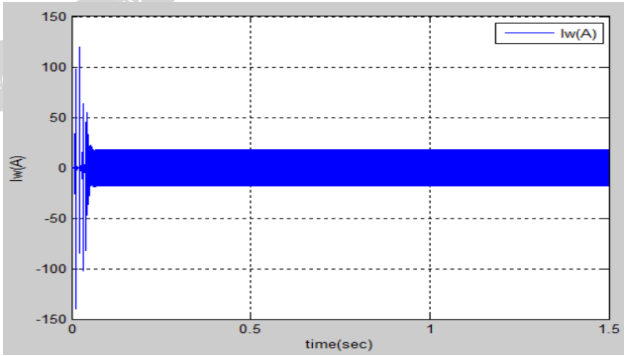


(g)

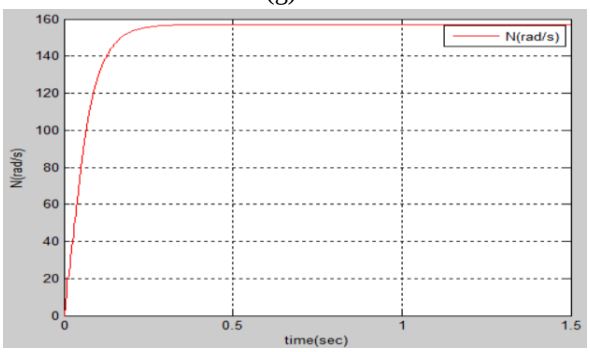


 DOI : 10.35291/2454-9150.2021.0414 © 2021, IJREAM All Rights Reserved.

(h)

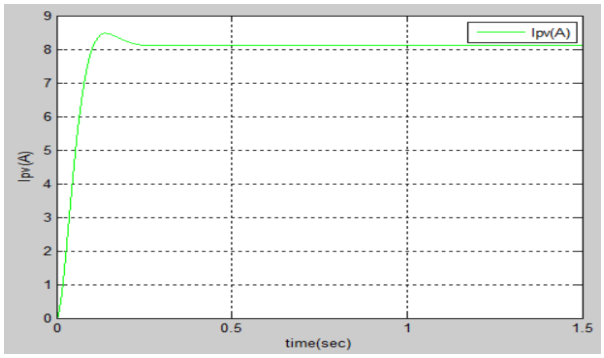


(i)

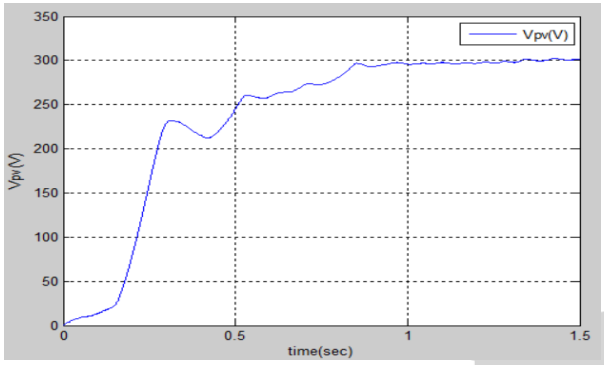


(j)

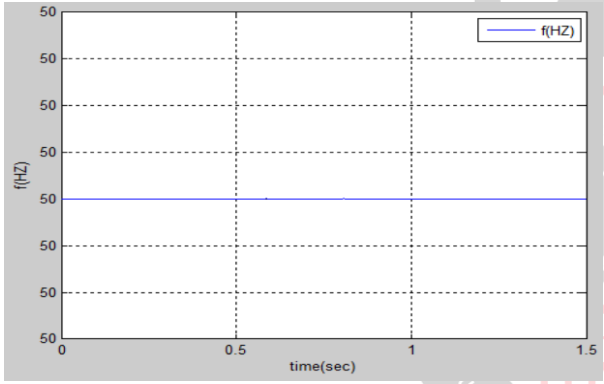


(k)

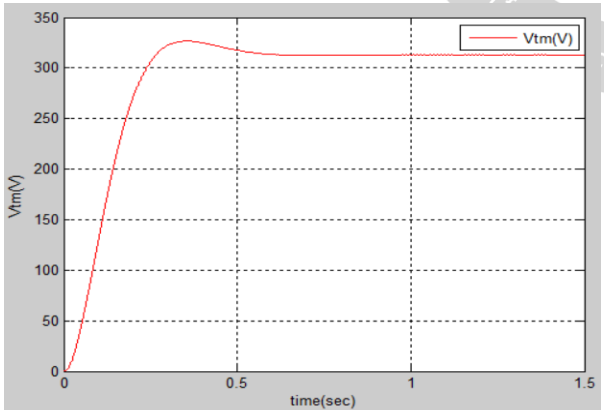


(l)

**Fig. 10(a) "(a-i)" Performance of DGS in simulation grid synchronization**

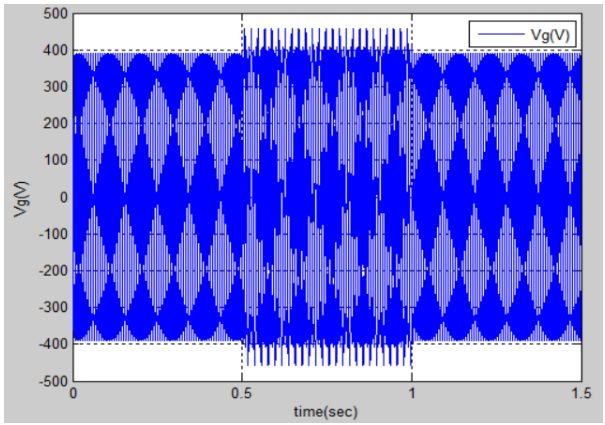


(a)

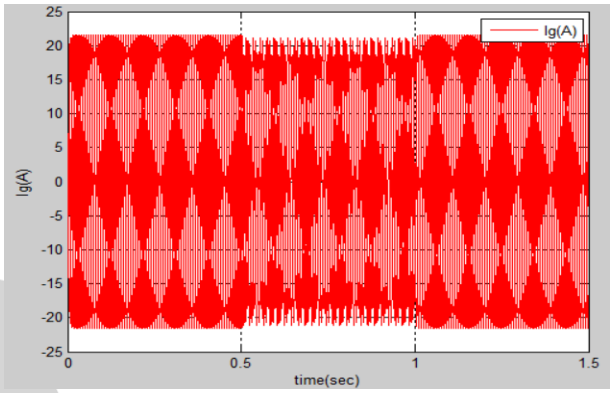


(b)

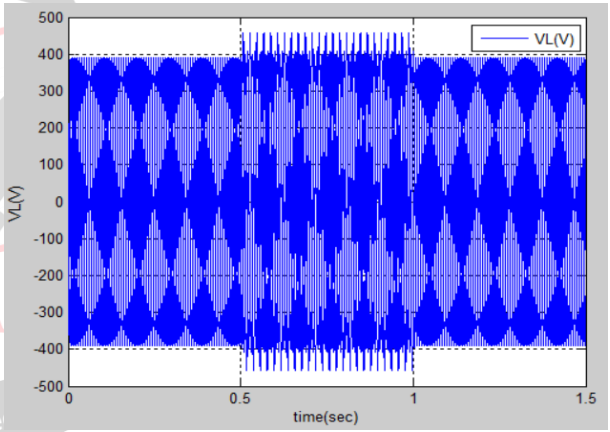


(c)

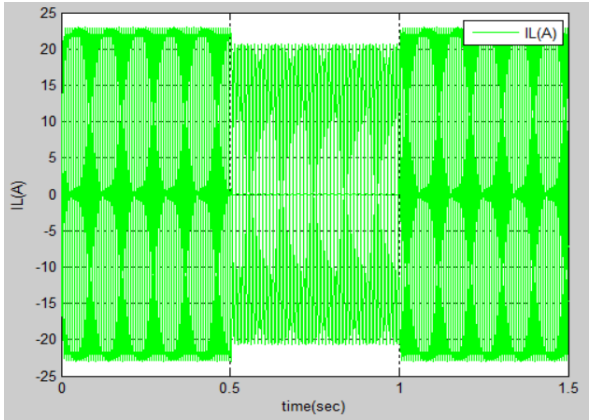


(d)

 DOI : 10.35291/2454-9150.2021.0414 © 2021, IJREAM All Rights Reserved.

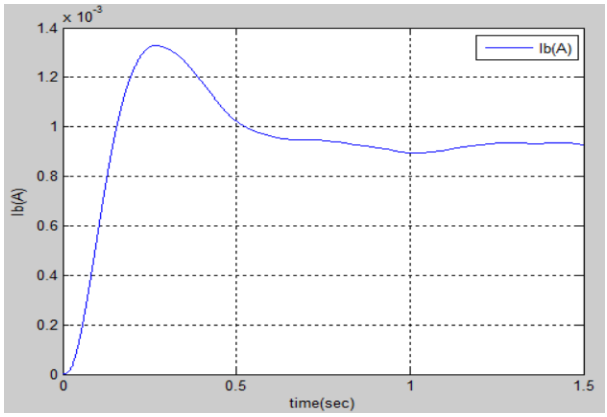


(e)

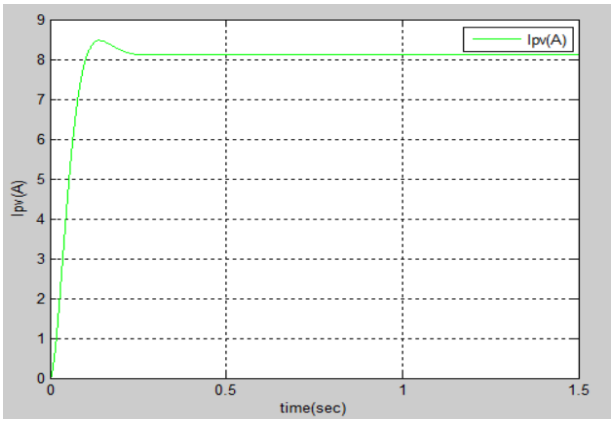


(i)

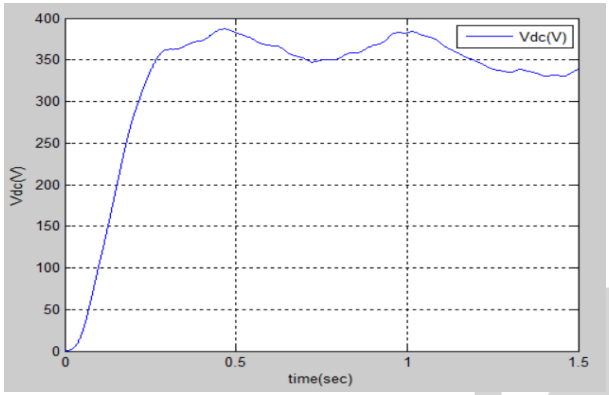


(f)

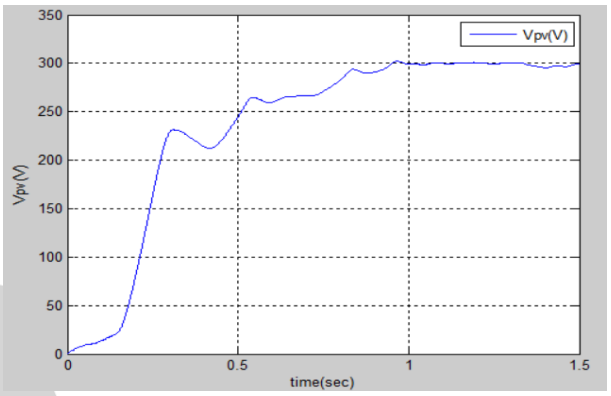


(j)

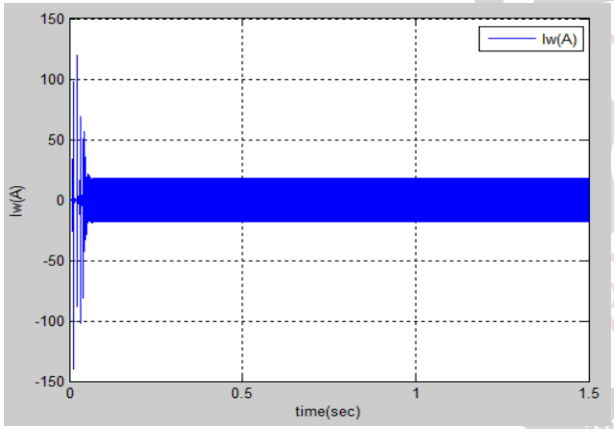


(g)

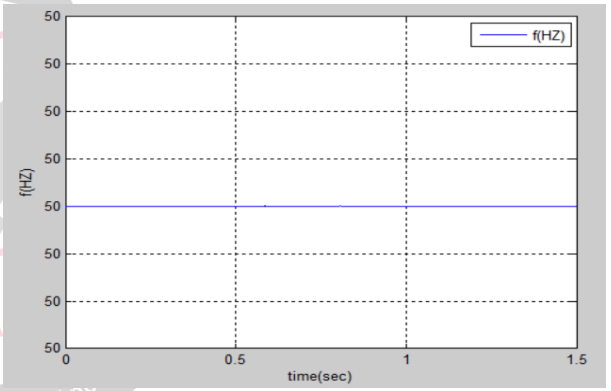


(k)

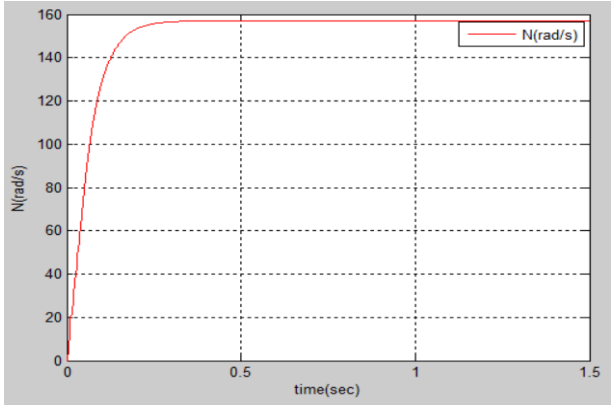


(h)

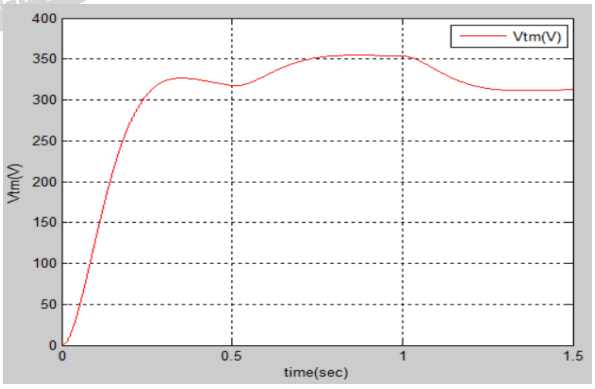


(l)

**Fig. 10(b) "(a-i)"Performance of DGS in simulation load unbalanced**

 DOI : 10.35291/2454-9150.2021.0414 © 2021, IJREAM All Rights Reserved.

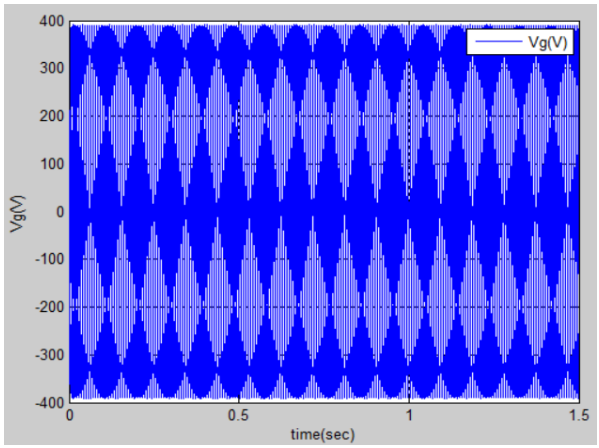


(a)

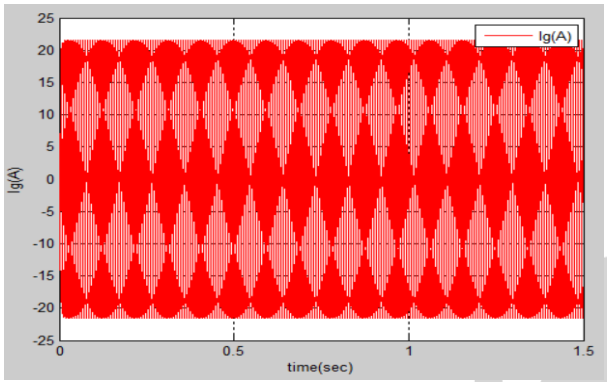


(b)

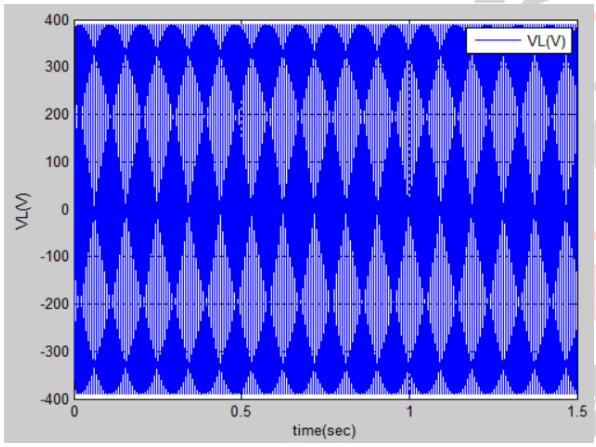


(c)

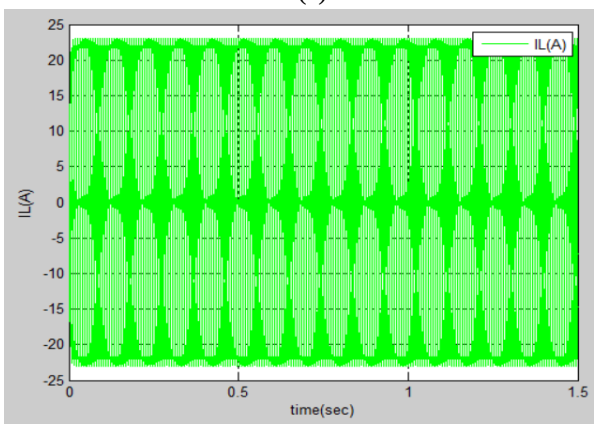


(d)

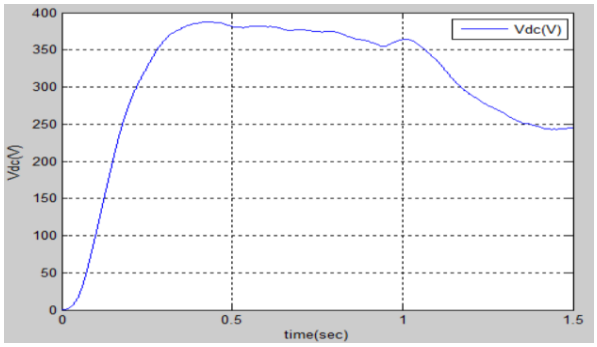


(e)

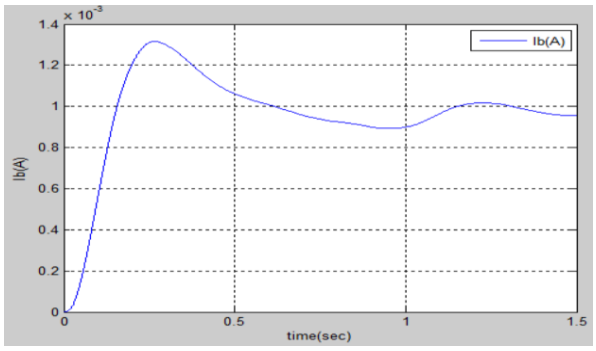


(f)

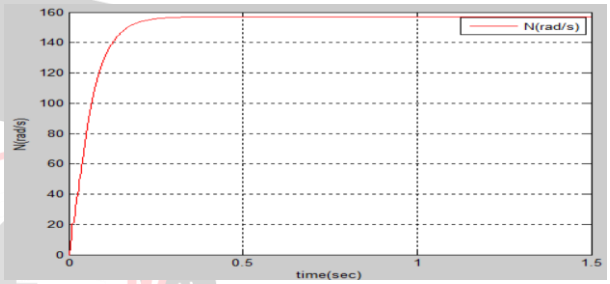


(g)

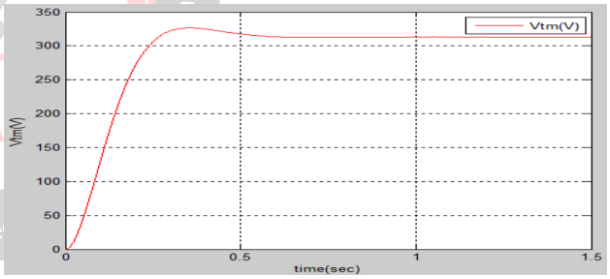


(h)

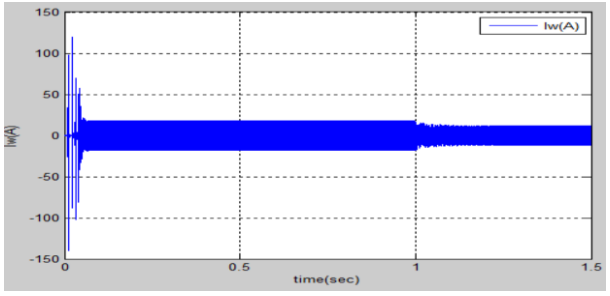


(i)

 DOI : 10.35291/2454-9150.2021.0414 © 2021, IJREAM All Rights Reserved.

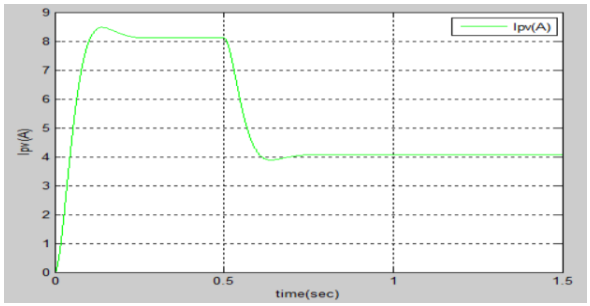


(j)

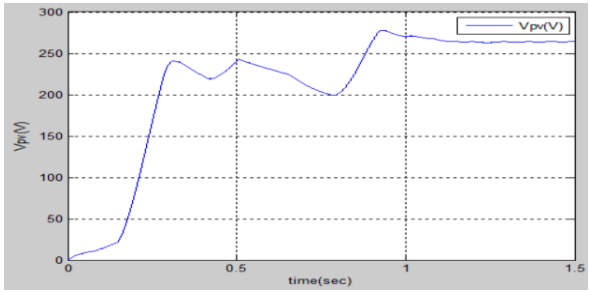


(k)

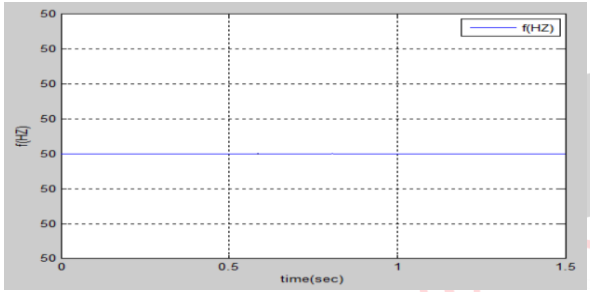


(l)

**Fig. 10(c) "(a-i)" Performance of DGS in simulationsolar insolation and wind speed variation**

## VI. CONCLUSION

Performance of micro grid that includes solar PV array and wind energy generating system with BES, is validated with the use of appropriate control schemes on a prototype developed in the laboratory. The DGS has been shown in many modes of operation, including islanded mode and grid connected mode with switching mode. The performance of the system is found effective for steady state and dynamic conditions including changing wind speeds, varying solar insulation level and load unbalanced conditions. The results of the tests demonstrate the robustness of the control approach, which can work in grid linked mode. Moreover, the transient free mode change is also presented through test results. The results have demonstrated the performance of DGS at The MSVSC control using FLC adapted PI speed controller, provides fast tracking of the control signal with less overshoot, reduced settling time and with less oscillations. Different dynamic conditions and validated the robustness and effectiveness of control. The usefulness of the feed-forward term in the grid connected mode, as well as the smooth operation of the grid connected mode during a battery disconnection, was also demonstrated in the tests.

## REFERENCES

[1] Nikoobakht, J. Aghaei, M. Shafie-khah and J. P. S. Catalão, "Assessing Increased Flexibility of Energy Storage and Demand Response to Accommodate a High Penetration of Renewable Energy Sources," IEEE Trans. on Sus. Energy, Early Access, 2018.

[2] B. Celik, S. Suryanarayanan, R. Roche and T. M. Hansen, "Quantifying the Impact of Solar Photovoltaic and Energy Storage Assets on the Performance of a Residential Energy Aggregator," IEEE Trans. Sus. Energy, Early Access, 2018.

[3] G. Delille, B. Francois and G. Malarange, "Dynamic Frequency Control Support by Energy Storage to Reduce the Impact of Wind and Solar Generation on Isolated Power System's Inertia," IEEE Trans. on Sust. Energy, vol. 3, no. 4, pp. 931-939, 2012.

[4] I. Alsaidan, A. Khodaei and W. Gao, "Determination of battery energy storage technology and size for standalone microgrids," in Proc. of IEEE, PESGM, 2016, pp. 1-5.

[5] U. Datta, A. Kalam and J. Shi, "Battery Energy Storage System Control for Mitigating PV Penetration Impact on Primary Frequency Control and State-of-Charge Recovery," IEEE Trans. Sus. Energy, Early Access, 2018.

[6] Z. Yi, W. Dong and A. H. Etemadi, "A Unified Control and Power Management Scheme for PV-Battery-Based Hybrid Microgrids for Both Grid-Connected and Islanded Modes," IEEE Trans. on Smart Grid, vol. 9, no. 6, pp. 5975-5985, 2018.

[7] M. Jafari, Z. Malekjamshidi, J. Zhu and M. Khooban, "Novel Predictive Fuzzy Logic-Based Energy Management System for Grid-connected and Off-grid Operation of Residential Smart Micro-grids," IEEE Jou. of Emer. and Sele. Top. in Power Elect. Early Access, 2018.

[8] G. G. Talapur, H. M. Suryawanshi, L. Xu and A. B. Shitole, "A Reliable Microgrid with Seamless Transition Between Grid Connected and Islanded Mode for Residential Community With Enhanced Power Quality," IEEE Trans. on Indu. Appl., vol. 54, no. 5, pp. 5246-5255, 2018.

[9] S. Adhikari and F. Li, "Coordinated V-f and P-Q Control of Solar Photovoltaic Generators with MPPT and Battery Storage in Microgrids," IEEE Trans. on Sm. Grid, vol. 5, no. 3, 2014.

[10] Q. Wu, E. Larsen, K. Heussen, H. Binder and P. Douglass, "Remote Off-Grid Solutions for Greenland and Denmark: Using smart-grid technologies to ensure

 DOI : 10.35291/2454-9150.2021.0414 © 2021, IJREAM All Rights Reserved.

secure, reliable energy for island power systems," IEEE Electri. Magazine, vol. 5, no. 2, pp. 64-73, 2017.

[11] S. S. Thale and V. Agarwal, "Controller Area Network Assisted Grid Synchronization of a Microgrid With Renewable Energy Sources and Storage," IEEE Trans. on Sm. Grid, vol. 7, no. 3, pp. 1442-1452, 2016.

[12] A. B. Shitole, Girish G. Talapur ,Shelas Sathyan, Makarand S. Ballal, Vijay B. Borghate, Manoj R. Ramteke, Madhuri A. Chaudhari, "Grid Interfaced Distributed Generation System With Modified Current Control Loop Using Adaptive Synchronization Technique," IEEE Trans. Ind. Infor., vol. 13, no. 5, pp. 2634-2644, 2017.

[13] D. Yazdani, A. Bakhshai, G. Joos and M. Mojiri, "A Nonlinear Adaptive Synchronization Technique for Grid-Connected Distributed Energy Sources," IEEE Trans. Power Elect., vol. 23, no. 4, pp. 2181-2186, 2008.

[14] H. A. Hamed, A. F. Abdou, E. E. El-Kholy and E. H. E. Bayoumi, "Adaptive cascaded delayed signal cancelation PLL based fuzzy controller under grid disturbances," in Proc. of IEEE MWSCAS, 2016.

[15] A. Bouhouta, S. Moulahoum, N. Kabache and I. Colak, "Experimental Investigation of Fuzzy Logic Controller Based Indirect Current Control Algorithm for Shunt Active Power Filter," in Proc. of IEEE International Conference on Renewable Energy Research and Applications (ICRERA), Brasov, Romania, 2019, pp. 309-314.

[16] W. Libo, Z. Zhengming and L. Jianzheng, "A Single-Stage Three-Phase Grid-Connected Photovoltaic System With Modified MPPT Method and Reactive Power Compensation," IEEE Trans. Energy Conversion, vol. 22, no. 4, pp. 881-886, Dec. 2007.

[17] K. Vishal and V. R., "An Improved SRF-Theory Based Controller Applied to Three Phase Grid Interfaced PV-System for Power Quality Improvement and Islanding Detection," in Proc. of IEEE Innovative Smart Grid Tech. - Asia (ISGT Asia), Singapore, 2018, pp. 740-745.

[18] P. Chittora, A. Singh and M. Singh, "Adaptive EPLL for improving power quality in three-phase three-wire grid-connected photovoltaic system," IET Rene. Power Gene., vol. 13, no. 9, pp. 1595-1602, 8 7 2019.

[19] A. Bendib, A. Chouder, K. Kara, A. Kherbachi and S. Barkat, "SOGI-FLL Based Optimal Current Control Scheme for Single-Phase Grid-Connected Photovoltaic VSIs with LCL Filter," in Proc. of IEEE International Conference on Electrical Sciences and Technologies in Maghreb (CISTEM), Algiers, 2018.

[20] F. Xiao, L. Dong, L. Li and X. Liao, "A Frequency-Fixed SOGI-Based PLL for Single-Phase Grid-Connected Converters," IEEE Tran. on Power Electr., vol. 32, no. 3, pp. 1713-1719, March 2017.

[21] T. Ngo, Q. Nguyen and S. Santoso, "Improving performance of single-phase SOGI-FLL under DC-offset voltage condition," in Proc. of IEEE IECON 2014 , Dallas, TX, 2014, pp. 1537-1541.

[22] F. Huang, J. Zhang and S. Zhang, "Affine Projection Versoria Algorithm for Robust Adaptive Echo Cancellation in Hands-Free Voice Communications," IEEE Trans. on Veh. Tech., vol. 67, no. 12, pp. 11924-11935, 2018.

[23] S. Kewat and B. Singh, "Grid Synchronization of WEC-PV-BES Based Distributed Generation System using Robust Control Strategy," in Proc. of IEEE Ind. Appl. So. An. Meet., Baltimore, MD, USA, 2019, pp. 1-8.

[24] S. Pradhan, B. Singh, B. K. Panigrahi and S. Murshid, "A Composite Sliding Mode Controller for Wind Power Extraction in Remotely Located Solar PV–Wind Hybrid System," IEEE Trans. Ind. Elect., vol. 66, no. 7, pp. 5321-5331, July 2019.

[25] F. Chishti, S. Murshid and B. Singh, "Development of Wind and Solar Based AC Microgrid With Power Quality Improvement for Local Nonlinear Load Using MLMS," IEEE Trans. Industry Applications, vol. 55, no. 6, pp. 7134-7145, Nov.-Dec. 2019.

[26] B. Singh, F. Chishti and S. Murshid, "Disturbance Rejection Through Adaptive Frequency Estimation Observer for Wind-Solar Integrated AC Microgrid," IEEE Trans. Ind. Inf, vol.15, no.11, pp. 6035-6047, 2019.

[27] P. S. Kumar, R. P. S. Chandrasena, V. Ramu, G. N. Srinivas and K. V. S. M. Babu, "Energy Management System for Small Scale Hybrid Wind Solar Battery Based Microgrid," IEEE Access,vol.8, pp.8336-8345, 2020.

[28] K. Kumar, N. Ramesh Babu and K. R. Prabhu, "Design and Analysis of RBFN-Based Single MPPT Controller for Hybrid Solar and Wind Energy System," IEEE Access, vol. 5, pp. 15308-15317, 2017.

[29] F. Chishti, S. Murshid and B. Singh, "LMMN-Based Adaptive Control for Power Quality Improvement of Grid Intertie Wind–PV System," IEEE Trans. Industrial Informatics, vol. 15, no. 9, pp. 4900-4912, Sept. 2019.

[30] S. Pradhan, S. Murshid, B. Singh and B. K. Panigrahi, "Performance Investigation of Multifunctional On-Grid Hybrid Wind–PV System With OASC and MAF-Based

 DOI : 10.35291/2454-9150.2021.0414 © 2021, IJREAM All Rights Reserved.

Control," IEEE Trans. Power Electronics, vol. 34, no. 11, pp. 10808-10822, Nov. 2019.

[31] A. A. A. Radwan and Y. A. I. Mohamed, "Grid-Connected Wind-Solar Cogeneration Using Back-to-Back Voltage-Source Converters," IEEE Trans. Sustainable Energy, vol. 11, no. 1, pp. 315-325, Jan. 2020.

[32] Y. M. Atwa, E. F. El-Saadany, M. M. A. Salama, R. Seethapathy, M. Assam and S. Conti, "Adequacy Evaluation of Distribution System Including Wind/Solar DG During Different Modes of Operation," IEEE Transactions on Power Systems, vol. 26, no. 4, pp. 1945-1952, Nov. 2011.

[33] S. L. Prakash, M. Arutchelvi and A. S. Jesudaiyan, "Autonomous PV-Array Excited Wind-Driven Induction Generator for Off-Grid Application in India," IEEE Journal of Emerging and Selected Topics in Power Electronics, vol. 4, no. 4, pp. 1259-1269, Dec. 2016.

[34] A. Parida and D. Chatterjee, "Model-based loss minimisation scheme for wind solar hybrid generation system using doubly fed induction generator," IET Elec. Pow. App.s, vol. 10, no. 6, pp. 548-559, 7 2016.

[35] M. Manohar, E. Koley and S. Ghosh, "Stochastic Weather Modeling-Based Protection Scheme for Hybrid PV–Wind System With Immunity Against Solar Irradiance and Wind Speed," IEEE Systems Journal.

[36] F. Giraud and Z. M. Salameh, "Steady-state performance of a grid-connected rooftop hybrid wind-photovoltaic power system with battery storage," IEEE Trans. Energy Con., vol. 16, no. 1, pp. 1-7, March 2001.

[37] S. Kumar Tiwari, B. Singh and P. K. Goel, "Design and Control of Microgrid Fed by Renewable Energy Generating Sources," IEEE Trans. Industry Applications, vol. 54, no. 3, pp. 2041-2050, May-June 2018.

[38] S. Teleke, M. E. Baran, S. Bhattacharya and A. Q. Huang, "Rule-Based Control of Battery Energy Storage for Dispatching Intermittent Renewable Sources," IEEE Trans. Sust. Ene., vol. 1, no. 3, pp. 117-124, Oct. 2010.

[39] R. G. Wandhare and V. Agarwal, "Novel Integration of a PV-Wind Energy System with Enhanced Efficiency," IEEE Trans. Power Electronics, vol. 30, no. 7, pp. 3638-3649, July 2015.

[40] B. Mangu, S. Akshatha, D. Suryanarayana and B. G. Fernandes, "Grid-Connected PV-Wind-Battery-Based Multi-Input Transformer-Coupled Bidirectional DC-DC Converter for Household Applications," IEEE Journal of Emerging and Selected Topics in Power Electronics, vol. 4, no. 3, pp. 1086-1095, Sept. 2016.

[41] A. Chatterjee and D. Chatterjee, "An Improved Current Balancing Technique of Two-Winding IG Suitable for Wind-PV-Based Grid-Isolated Hybrid Generation System," IEEE Systems Journal.

[42] C. Bhattacharjee and B. K. Roy, "Advanced fuzzy power extraction control of wind energy conversion system for power quality improvement in a grid tied hybrid generation system," IET Generation, Transmission & Distribution, vol. 10, no. 5, pp. 1179-1189, 7 4 2016.

## AUTHORS PROFILE

K.G.Ravi Krishna is an Under Graduate student studying IV B.Tech Electrical and Electronics Engineering from JNTU Anantapur at Chadalawada Ramanamma Engineering College(Autonomous), Tirupati, Andhra Pradesh, India. His areas of interest power system and power electronics.

Dr.J.Srinu Naick received his B.E degree in Electrical & Electronics Engineering from Andhra University Vishakhapatnam AP, India in 2003 and M.Tech with Energetics from NIT Calicut, Calicut, and Kerala, India in 2007. Ph.D with power system from Achiryanagarjuna university in 2019 He is having 17 years of teaching and research experience. He is currently working as Professor in the Department of EEE, Chadalawada Ramanamma Engineering college(Autonomous), JNTUA, Tirupati, Andhra Pradesh, India. His areas of interest are in the Power systems Industrial Drives & FACTS Controllers.

 DOI : 10.35291/2454-9150.2021.0414 © 2021, IJREAM All Rights Reserved.